

Dynamic Monitoring of the Rat Uterus Using 3D Automatic Segmentation

E. Eyal¹, A. Akselrod-Ballin², M. Galun², E. Furman-Haran¹, C. Gunanathan³, R. Basri², A. Brandt², D. Milstein³, H. Degani²

¹Biology Regulation, Weizmann Institute of Science, Rehovot, Israel, ²Computer Science and Applied Math, Weizmann Institute of Science, Rehovot, Israel, ³Organic Chemistry, Weizmann Institute of Science, Rehovot, Israel

Purpose:

To develop a 3D MRI automatic segmentation of the rat uterus as a tool for quantitative analysis of a new Estrogen Receptor-MR contrast agent conjugate.

Introduction:

The activity of the uterus is predominantly regulated by the steroids hormones, estrogen (E₂) and progesterone. Hence, this organ serves as a classical model for endocrine studies of the steroid receptors mechanism. Current uterine experiments usually involve morphological, physiological, biochemical and molecular characterization performed by sacrificing the animals and extracting uterine tissues. Developing of non-invasive imaging techniques to monitor the uterus *in vivo* allow continuous spatial and temporal follow up on the same animal model and enhance precision as well as reproducibility. Indeed, magnetic resonance imaging (MRI) offers high spatial resolution, soft tissue contrast and multiple novel contrast mechanisms which can be simultaneously exploited. However, MRI is also susceptible to artifacts such as field inhomogeneity, chemical-shift, partial volume, motion and folding. To overcome part of these problems we present here a protocol for a high resolution and fast acquisition of uterine MR images and an automatic method to create a 3D (volumetric) structure of the uterus in the intact rat. The rat positioning, anesthesia procedure and MRI acquisition protocol were optimized to minimize artifacts and enhance contrast between the uterus and other abdominal organs. We have introduced a novel 3D multi-channel multiscale automatic segmentation algorithm, and applied it to automatically extract the uterus region of interest (ROI). Utilizing this method we were able to achieve high contrast between the uterus and other abdominal organs and observe the inner structure of the rat uterus. Both single and multi-channel automatic segmentation demonstrated high correlation to a manual segmentation. The algorithm produced a full hierarchy of segments in time that is linear in the dataset size, essential for multi-channel 3D medical experiments. We further used this segmentation method to analyze a contrast enhanced MRI experiments of a novel contrast agent composed of an estrogenic part tagged to a new pyridinium based gadolinium chelate (E₂-Pyr-Gd) that demonstrated a r₁ relaxivity in buffer solution of 7.9 s⁻¹mM⁻¹ and has high binding affinity to the estrogen receptor.

Methods:

Animals: Female, ovariectomized, LEW/NHSD rats (6-8 month) were injected with 17-β-estradiol 48h before the experiment. During the MRI experiments, rats were anesthetized by inhalation of 1.5% Isoflurane in an O₂:N₂O (3:7) mixture, applied through a nose cone. All animal procedures were approved by the Weizmann Institute's Animal Care and Use Committee.

MRI: MR images were recorded with a 4.7 T/30 cm bore Biospec spectrometer (Bruker, Germany), equipped with a ¹H radio frequency coil with an inner diameter of 7.5 cm. Coronal MR images tilted in 10° covering the whole abdominal cavity were acquired with the following protocols: (1) T₁-weighted, 3D gradient echo with TE/TR of 4.3/18.3 ms; a 30° flip angle. (2) T₂ weighted (T2w) 2D rapid spin echo (RARE) with TE/TR of 47.2/3200 ms, a rare factor of 4. (3) Proton density weighted (PDw), 2D fast low-angle shot gradient echo with TE/TR of 4.2/500 ms, 30° flip angle. The distribution of E₂-Pyr-Gd in the uterus was monitored by protocol 1 over a period of 6h after a bolus injection of E₂-Pyr-Gd into the tail vein at a dose of 0.024 mmol/kg body weight. Protocols 2 and 3 served for the segmentation process. The spatial resolution for all sequences was 0.27x0.27x0.5 mm³, using a matrix of 256x256. Fat suppression was used in all protocols by applying a 90° gauss shaped preparation pulse 700Hz off resonance (SW of 600Hz) followed by a dephasing gradient.

Segmentation: The algorithm is an extension of the 2D multiscale segmentation algorithm developed for natural images [1,2&4]. The algorithm constructs a pyramid of graphs, which adaptively represents aggregates of pixels of similar properties. At fine levels these aggregates represent regions of homogenous intensities. At coarser levels the aggregates represent regions of coherent properties (such as intensity variations at various scales, texture measures, boundary continuation, etc.). Starting with the given image pixels at the finest level, each aggregate in every coarser level is constructed as a union of some next-finer-level aggregates. Based on the algebraic multigrid scheme [3] coarsening procedures, the aggregation is soft, i.e., each aggregate at fine levels may belong to several larger aggregates at coarser scales, with different weights. This weighted aggregation allows the algorithm to avoid local, pre-mature decisions. During the construction of the pyramid we collect statistics of the aggregates that include intensity, intensity variability, shape, and filter responses using these statistics to evaluate neighbor similarities. As a result of this process segments that are distinct from their surroundings emerge as salient nodes at a certain level of the pyramid. The algorithm produces a full hierarchy of segments in time that is linear in the dataset size which is essential for multi-channel 3D medical experiments. Single channel 3D segmentation was performed on the T2w channel (protocol 2) and multi-channel segmentation was performed by combining T2w and PDw channels (protocol 2 & 3), the segmentation result was refined by the use of morphological operator variant. To evaluate the algorithm performance, manual segmentation was performed for both channels separately and quantitative comparison based on common measures for spatial overlap was calculated.

Results & Discussion:

MR imaging: The T2w sequence distinctly allowed the delineation of the endometrium (Fig. 1a) and the PDw sequence captured the whole uterus, However, the latter sequence resulted in low contrast between the uterus and the intestine (Fig. 1b).

Segmentation: The segmented endometrial tissue derived from single channel T2w data was precisely extracted. The multi-channel segmentation calculated using the combined T2w and PDw images yield an ROI that covers most of the uterus volume regardless of the inner structure of the horns. The T2 weighted image served as a backbone for the segmentation, while the data derived from the PD image referred to the peripheral details (Fig. 1b). With our non optimal implementation, on 200 x 200 x 15 voxels the execution time for single- and multi-channel segmentation was 40 sec and 60 sec, respectively on a standard P4 3GHz PC. Quantitative correlation of the automatic and manual segmentations showed high degree of homology between the ROIs based on the automatic single- and multi-channel data and the corresponding ROIs derived by the manual segmentation (Table 1). Preliminary results of the dynamic distribution of E₂-Pyr-Gd using the segmentation method showed that it enters the various tissues, reaching a maximum level at about 0.5 h and then, gradually drains from the tissues to full clearance at about 4 h. However, in the uterine endometrial tissue, which expresses high estrogen receptor level, this agent remains at a constant level for the first 2.5h and only then drains out. These results suggest that E₂-Pyr-Gd binds to the ER in the endometrium and is immobilized there and then, due to the turn over of ER (the half-life of ER is 3 h), is cleared out.

Conclusions:

We present a protocol for high resolution and fast acquisition of MR images of *in vivo* rat uterine tissues and an algorithm for the accurate automatic calculation of the uterus boundaries and its 3D structure. We demonstrate the utilization of the single and multi channel segmentation algorithm in dynamic contrast enhanced studies. The segmentation algorithm can be further applied for other medical imaging tasks while incorporating multi feature or multi-channel data.

References: 1. E. Sharon *et al.* IEEE 1:469-476, 2001 2. M. Galun *et al.* ICCV, 1:716--723, 2003. 3. A. Brandt *et al.* Inst. for Computational Studies, POB 1852, Fort Collins, Colorado, 1982. 4. A. Akselrod-Ballin *et al.* submitted to cvpr'06

Work supported by: DOA/BC 044499; NIH/CA 42238 and Lord David Alliance, UK.

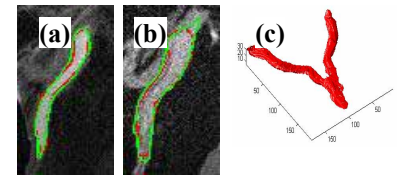


Fig 1: The automatic (green) and manual (red) segmentation boundaries for (a) endometrium placed on T2w image, (b) entire uterus placed on PDw image and (c) example for 3D automatic uterus ROI.

	$(S \cap R)/ R $	$2* S \cap R /(S + R)$
Endometrial segmentation based on single-channel T2w	0.9±0.02	0.89±0.02
Entire uterus segmentation based on Multi-channel	0.89±0.02	0.85±0.03

Table1: Quantitative comparison between the automatic (S) and the manual (R) segmentation, averaged over 5 structures.